International Journal of Applied Earth Observation and Geoinformation 24 (2013) 1–8

Contents lists available at SciVerse ScienceDirect

International Journal of Applied Earth Observation and Geoinformation

journal homepage: www.elsevier.com/locate/jag

Estimating the Leaf Area Index, height and biomass of maize using HJ-1 and RADARSAT-2

Shuai Gao[a,*], Zheng Niu[a], Ni Huang[a,b], Xuehui Hou[a,b]

[a] The State Key Laboratory of Remote Sensing Science, Institute of Remote Sensing and Digital Earth, Chinese Academy of Sciences, Beijing 100101, China
[b] University of Chinese Academy of Science, Beijing 100039, China

ARTICLE INFO

Article history:
Received 20 June 2012
Accepted 6 February 2013

Keywords:
Leaf Area Index
Height
Biomass
Vegetation indices (VIs)
HJ-1
RADARSAT-2

ABSTRACT

New optical and microwave integrated vegetation indices (VIs) were designed based on observations from both field experiments and satellite (HJ-1 and RADARSAT-2) data. It was found that these VIs perform better in estimating the structure parameters of maize, such as Leaf Area Index (LAI), height and biomass, than the original ones. This investigation focused on the difference of interaction between the multispectral reflectance and microwave backscattering signatures with the maize growth variables. Because the maize was near the heading stage with large vegetation coverage in the experiment, the reflectance of the near-infrared band of HJ-1 was much less sensitive to the structure variables than that of the visible-light band. Thus, the optical VIs formulated using those bands were saturated to estimate the structure parameters. With respect to the RADARSAT-2 data, there was a relatively strong relationship between the HV cross-polarization and the volume scattering of the maize, which was mostly determined by the crown structure. The modified VIs were designed using both the VIs of HJ-1 and the HV cross-polarization of RADARSAT-2 to overcome the saturation limitation. The validation showed that this integrated method of determining VIs is a good alternative to that using only the optical or microwave observation.

1. Introduction

The accurate estimation of vegetation biochemical and biophysical variables is important in many agricultural, ecological, and meteorological applications (Darvishzadeh et al., 2008). Three of these variables—Leaf Area Index (LAI), height, and biomass—can be used to describe the architecture of plants, monitor changes in canopy structure, and predict growth and yield. The reliable estimation of these variables during the growing season would improve planning, the management of grain production, the handling of the grain, and marketing (Dente et al., 2008). Moreover, because these variables vary seasonally and respond rapidly to stress factors and changes in climatic conditions, it is important to estimate their values frequently, but this can be difficult when the vegetation covers large areas.

Due to its ability to collect information over regional and global scales, remote sensing is the only reasonable method that can be used to estimate these variables over large areas. Plant stand architecture is the dominant factor responsible for the spectral reflectance of vegetative canopies in the visible and near-infrared (NIR) spectrum, and studies show that there are fairly strong correlations between these parameters and spectral vegetation indices (VIs) using various combinations of visible, NIR, and shortwave reflectance (Chen and Cihlar, 1996; Chen et al., 1997). However, methods based solely on optical data will always have some limitations because the vegetation indices lose accuracy for dense canopies when the LAI exceeds 2–5 for some crops (Haboudane et al., 2004; Tang et al., 2007). Moreover, the use of optical data is restricted by the requirement of cloud-free daylight conditions.

Similarly, in most agricultural applications, space-borne remote sensing is a common tool for analyzing large-scale landscape vegetation dynamics, which can include analyzing land cover, land use change, productivity, and disturbances (Frolking et al., 2009). However, passive optical remote sensing of crops can be obscured by frequent cloud cover and by significant atmospheric aerosol interference during the dry season (Zhao et al., 2005). SAR is much less sensitive to atmospheric moisture and aerosols than optical sensors (Ulaby et al., 1986), and it has the advantage of dense vegetation detection. For example, for maize near the heading period, most of the C-band backscattering of vegetation is known to come from canopies and not from the ground, especially at high incidence angles, which is based on its relatively low sensitivity to soil moisture (Ulaby et al., 1984; Inoue et al., 2002). However, SAR observation is limited by its imaging geometry and radiation mechanism. Therefore, it is urgently necessary to develop alternative approaches that ideally can be used in combination with the optical methods. In fact, this integration of optical and SAR observation has

* Corresponding author. Tel.: +86 1064806258.
E-mail address: gaoshuai@live.com (S. Gao).

0303-2434/$ – see front matter © 2013 Elsevier B.V. All rights reserved.
http://dx.doi.org/10.1016/j.jag.2013.02.002

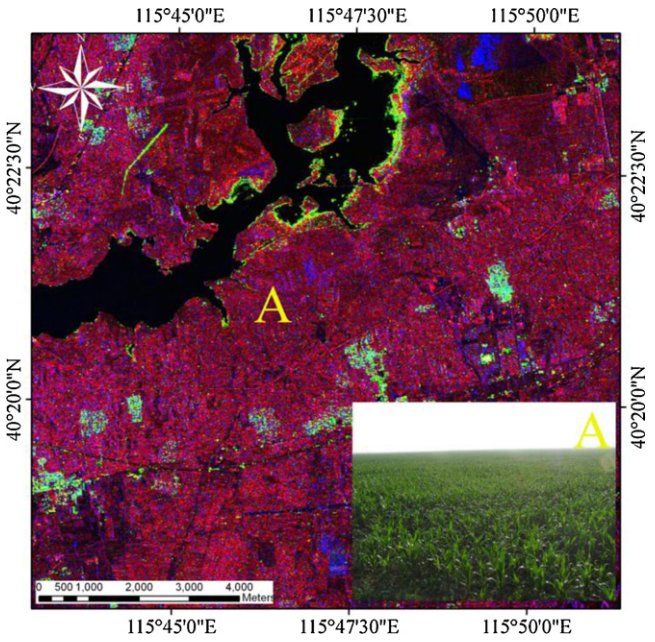

Fig. 1. The location of study area (RADARSAT-2 image after Freeman–Durden three-component decomposition).

been used for the LAI estimation of crops and forests; and in some cases, the results have been closer to the actual values (Clevers and Vanleeuwen, 1996; Manninen et al., 2005a). This good agreement is due to the fact that optical observation can offer an accurate interpretation of photosynthesis and non-photosynthesis components of plants and SAR is much more sensitive to plant structure and soil moisture, both of which reflect the growing status of vegetation.

In this analysis, high-resolution SAR data (RADARSAT-2) combined with optical data (HJ-1) were used to retrieve crop (maize) structure parameters. Maize is an important food crop that is widely planted in northern China. Thus, monitoring its growing status and estimating its production has become increasingly necessary. However, optical and radar remote sensing have limitations in crop monitoring, especially with dense vegetation coverage. It is for this reason that this study aimed to improve the synergic use of optical and radar remote sensing data to improve the estimation accuracy of crop architecture parameters, such as LAI, height and biomass in the context of precision farming. The use of VIs for convenient crop monitoring has inspired the development and testing of modified VIs, which combine SAR data with optical data. Our aim is to present an integrated inversion method that simply and accurately determines the architecture parameters of crop canopies for agriculture management purposes.

2. Materials

2.1. Field experiments

Field experiments were carried out in the Huailai area (Fig. 1), 84 km north of Beijing, China. The test site was located in the flat area of the Huailai-Yanqing Basin, along the south of the Guanting Reservoir, which is dominated by maize. Most of the maize is sowed in late May, and flowering occurs near late July; the maize is harvested between mid-September and late September. Due to the influence of mountains to the north and a nearby reservoir, there are many foggy and cloudy days in summer. As a result, the active and passive remote sensing experiments were coordinated with the measurement of the optical reflectance and microwave backscattering characteristics of the vegetation. The field parameters of maize used in the study were investigated from 16 July to 18 July 2010, prior to the emergence of tassels. The field parameters measured included LAI, height, biomass, Leaf Water Area Index (LWAI), Leaf Area Density (LAD), Chlorophyll Content (CC, SPAD reading), and Leaf Water Content (LWC) (Table 1).

In the study site, there were 29 rectangular sample plots with a width and a length of at least 50 m. Most of the plots were ~6000 m^2 in area, with the smallest plot having an area >3000 m^2. All of the plots were used for correlation and sensitive analyses. The latitude and longitude of each plot was determined by Global Positioning System (GPS) measurements. LAI and LAD were measured using an LAI-2000 (LI-Cor Inc., Lincoln, Nebraska). In each measurement, three representative positions were chosen, and in every position, two repeated measurements were executed. For LAI and LAD, the mean values were calculated as reference values of each plot. The standard deviation (SD) for LAI within a plot varied from 0.1 to 0.2, with an average of 0.14. For LAD, the SD value varied from 1 to 5, with an average of ~3. For each plot, 5–10 representative maize plants were measured using a measuring tape to determine their mean height, and the average SD for these measurements was found to be ~8 cm. In addition, an SPAD-502 meter (Konic Minolta, Japan) was used to provide an instantaneous measurement of the leaf Chlorophyll Content; the SD for this measurement was ~4.9. Moreover, fresh leaf samples from each plot were weighed (fresh weight, F) and then oven-dried at 60 °C until a constant weight (dry weight, D) was reached. The value of LWC was calculated using Eq. (1). For LWC, the SD varied between 0.03 and 0.17, and the average value was 0.08.

$$\mathrm{LWC} = \frac{F - D}{F} \times 100\% \quad (1)$$

$$\mathrm{LWAI} = \mathrm{LAI} \times \mathrm{LWC} \quad (2)$$

$$\mathrm{Biomass} = 1.01 \times \mathrm{height} \times \exp(1.05 \times \mathrm{LAI}) \quad (R^2 = 0.88) \quad (3)$$

The value for LWAI was calculated using Eq. (2), based on the previous research of Dabrowska-Zielinska et al. (2007). Finally, the value for the biomass was calculated indirectly using Eq. (3), which was obtained by long-term observation of one maize field during the entire growing season of maize in this area (Fig. 2). The biomass consisted of the dry weight of leaves, stems, and roots.

Temperature, precipitation, and humidity data were recorded hourly using nearby weather stations (Table 2). There was almost no wind during those days. Unfortunately, soil moisture information was not collected from these plots during the study period. However, measurements in this area showed that the maize field soil was often dry during this period. The volumetric water content was obtained from long-term observation of the maize field using a TDR instrument (HydroSense, CAMPBELL), and the results were ~10% in 5 cm, ~12% in 10 cm, and ~15% in 20 cm.

Table 1
Statistics of the measured parameters in the 29 plots.

	LAI	Height (cm)	Biomass (g/m^2)	LWAI	LAD	CC	LWC
Min	1.17	44	246.97	0.57	32	39.43	0.46
Max	3.44	180.4	6526.25	2.15	62	57.80	0.65
Mean	2.22	121.76	1806.55	1.27	46.28	48.9	0.57
SD	0.64	35.23	1467.95	0.42	6.5	4.66	0.05

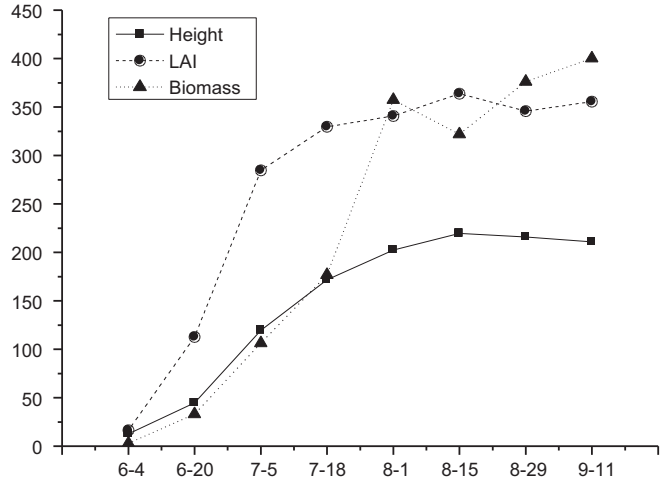

Fig. 2. Variation of height, LAI and biomass observed in one maize plot of this area (unit: height, cm; LAI, 0.01 m^2/m^2; biomass, 10 g/m^2).

Table 2
Weather conditions during the in situ field investigation and the dates the images were acquired at weather stations near the test site.

Date	Temperature at 2 m height (°C)	Precipitation per 24 h (mm)	Humidity (%)
July 16, 2010	24.1	0	85
July 17, 2010	24.8	2.6	80.5
July 18, 2010	25.2	0	79.5
July 20, 2010	24.3	0	77.5
July 25, 2010	27.6	0	78.5

2.2. Satellite data process

Two satellite images were used in this experiment: a multispectral image (HJ-1) collected on July 20, 2010 and a RADARSAT-2 image collected on July 25, 2010 (Table 3).

The HJ-1 image (path 4, row 64), which covered the entire Huailai test site, was provided by the China Center for Resources Satellite Data and Application (CRSDA); the image was acquired at a solar zenith angle of 64.15°. Radiometric corrections were made using coefficients provided with the image (e.g., gains and offsets). Then MOTRAN 4 model, which is embedded in the ENVI/FLAASH module, was applied for atmosphere correction. The input parameters were set based on the location, sensor type and ground weather conditions observed on the day the image was acquired. Then, the surface reflectance of the HJ-1 image was derived. Based on the ground control points selected from the registered SPOT image, the HJ-1 image was geometrically corrected to improve the accuracy of pixel registration to within one pixel (30 m). Each plot was corrected by approximately ~7–9 pixels to match the ground measurements.

The RADARSAT-2 fine-pol single-look complex (SLC) image was acquired on July 25, 2010. It had 50 km × 50 km swaths with a mean incidence angle of 37° in ascending passes. The SAR image was radiometrically calibrated to obtain the linear radar backscatter coefficient (σ^0) transformed from the digital number (DN) (Macdonald, 2008). To compensate for speckle noise, the boxcar filter was applied to replace the central pixel of a moving window (3 × 3 pixels) with the average value for the pixels in the window. This replacement was effective in reducing the speckle noise in homogeneous areas and preserving the mean value (Johnstone and Raimondo, 2004; Lee and Pottier, 2009). The mean backscattering coefficients were calculated from the calibrated SAR image by averaging the linear radar backscatter coefficient (σ^0) of all pixels within the field. For each plot, there were ~200 pixels participating within one average. The image was then rectified using a preprocessed SPOT image with a root mean square error of ~1 pixel. The terrain of the Huailaitest site considered in this study is comparatively flat; thus, the digital elevation model was not used in the rectification. The pixel size of the rectified image was similar to the pixel size of the original image to avoid losing or duplicating pixels.

3. Methods

In the first stage of this research, the relationship between the features of the satellite images and several measurements of plant variables (e.g., LAI and height) was examined using correlation analysis. The features of the satellite image included the reflectance and VIs of HJ-1 and the backscattering coefficients of RADARSAT-2. The aim of this study was to explore the sensitivity of the HJ-1 and RADARSAT-2 satellite sensors to the architecture parameters of maize. The advantages and limitations of each sensor were then analyzed based on ground measurement data. Freeman–Durden three-component decomposition (Freeman and Durden, 2002) was carried out to analyze the scattering contribution from the different maize components, in addition to the correlation between these three-components and the measured plant variables.

4. Results

4.1. Correlation analysis between reflectance and plant variables

It has been shown that reflectance at different wavelengths is related to the architecture parameters of vegetation crowns and other biochemical features (Jacquemoud and Baret, 1990; Daughtry et al., 2000). Thus, the correlation coefficients for LAI, height, biomass, and LWAI were calculated for all of the reflectance bands in the HJ-1 image. There was a negative correlation coefficient ($r = \sim -0.6$) between these parameters in the visible-light region, whereas there was a positive correlation ($r = \sim 0.5$) between these variables in the near-infrared region.

However, it has also been shown that different satellites exhibit different sensitivities. Therefore, the correlation between the vegetation parameters and other VIs—including the Ratio Vegetation Index (RVI) (Jordan, 1969), the Normalized Difference Vegetation Index (NDVI) (Tucker, 1979), and the Enhanced Vegetation Index

Table 3
Detailed information regarding the two satellite images used in the study.

Spectral region (μm)	Spatial resolution (m)	Orbit altitude (km)	Swath (km)	Date
HJ-1				
B1: 0.43–0.52B2: 0.52–0.60B3: 0.63–0.69B4: 0.76–0.90	30	649	360	July 20, 2010

Beam mode	Resolution range × azimuth (m)	Mean incidence angle	Pass	Date
RADARSAT-2				
Fine quad-pol (HH, HV, VH, VV)	5.2 × 7.6	37	Ascend	July 25, 2010

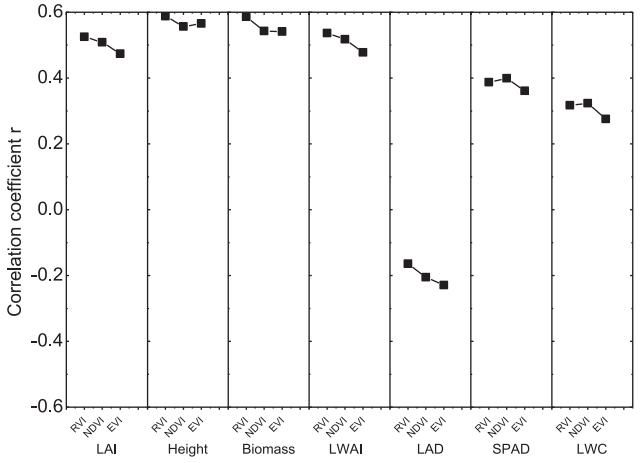

Fig. 3. Relationships between the vegetation determined indices using an image from HJ-1 and maize variables (LAI, Leaf Area Index; height, total biomass; LWAI, Leaf Water Area Index; LAD, Leaf Area Density; CC, Chlorophyll Content; LWC, Leaf Water Content) during this experiment (RVI, Ratio Vegetation Index; NDVI, Normalized Difference Vegetation Index; EVI, Enhanced Vegetation Index).

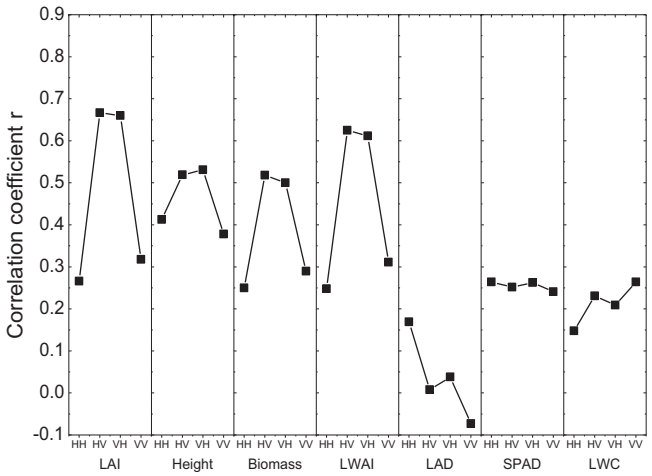

Fig. 4. Relationships between backscattering coefficients of RADARSAT-2 and maize variables. The HH, HV, VH, and VV represent the four different linear polarizations types.

(EVI)(Huete et al., 1997)—were analyzed to reduce the absolute reflectance calibration error. For each plot, the VI value of each pixel was calculated from the reflectance of the HJ-1 image; then, all of the VI pixel values were averaged to correlate with the vegetation parameters. The positive correlation coefficients were found using the RVI for the LAI ($r = 0.47$, SD = 0.04), height ($r = 0.59$, SD = 0.13), biomass ($r = 0.59$, SD = 0.13) and LWAI ($r = 0.54$, SD = 0.14) variables. The NDVI and EVI presented similar correlation coefficients for these variables (Fig. 3).

In the analysis, the correlation between the plant growth variables themselves was carefully considered. The correlation coefficient between LAI and height was 0.92; it was 0.96 between LAI and biomass, 0.99 between LAI and LWAI, 0.8 between LAI and CC, and 0.65 between LAI and LWC. The LAI, height, biomass and LWAI mostly reflected the variation in canopy architecture. The CC and LWC reflected the leaf scale information. Thus, the high correlations between the reflectance characteristics and the plant variables suggested that multispectral HJ-1 was much more sensitive to canopy architecture than to the leaf scale parameters, which had been proved by many preceding studies using other multispectral satellites similar to HJ-1 (Lu et al., 2005; Dash et al., 2010).

4.2. Correlation analysis between backscattering coefficients and plant variables

Because the backscattering coefficients were related to the physical parameters of the target, such as the amount and structure of scattering elements and their dielectric constants, a correlation between plant variables and backscattering coefficients should be meaningful as long as the biological variables (e.g., LAI, biomass, and canopy height) are strongly linked to those physical parameters. Here, the original linear representation of backscattering coefficient, not the logarithm conversion, was used for convenient analysis and comparison.

For the LAI, the highest correlation coefficient was found for the cross-polarization HV ($r = 0.67$, SD = 0.003) (Fig. 4). The co-polarization involving HH and VV was less well correlated ($r = 0.27$, SD = 0.02 and $r = 0.32$, SD = 0.02 for HH and VV, respectively). Similar trends were found for other parameters, such as canopy height, biomass and LWAI. Inoue et al. (2002) found a very high correlation between the C-band backscattering at a cross-polarization incidence angle of 35° with LAI for rice in an experimental paddy field ($r^2 = 0.96$–0.97) (Tsukuba, Japan) using a multi-frequency polarimetric scatterometer. However, there were many more factors—aside from the vegetation variables—that affected the satellite SAR signals more than the ground scatterometer. Similar to the case of HJ-1, a low correlation was found between the backscattering coefficients and leaf level characteristics, such as CC and LWC. This low correlation may be due to the fact that at a specific growth stage, the concentration of these parameters showed little variation for the maize (Table 1), and the variation of the backscattering coefficients was mainly caused by the structure characteristics of the vegetation canopy.

In this analysis, several backscattering polarization ratios were also studied using the RADARSAT-2 data, including VV/HH, HV/HH, and HV/VV (Fig. 5). Because the absolute values of HV and VH were similar for the SAR data, only HV was used to represent cross-polarization. It was found that although there was some relationship between these polarization ratios and plant variables, no significant correlation was found between the HH/VV or HV-related ratios. The VV/HH ratio showed little change with increasing LAI in our experiment, and this phenomenon was coincident with the following simulation (Blaes et al., 2006). When comparing the correlation coefficients, the HV-related polarization ratios provided a small advantage over HH/VV. This advantage may be due to the fact that cross-polarization is more related to volume scattering from the plant canopy, and co-polarization is related to double-bounce

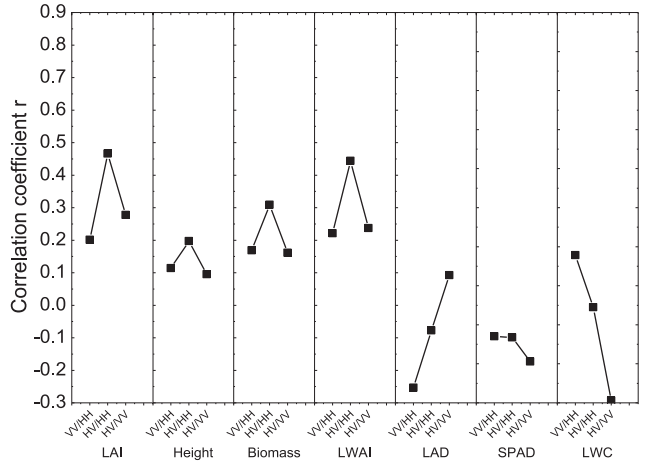

Fig. 5. Relationships between backscattering polarization ratio of RADARSAT-2 and plant variables. VV/HH, HV/HH, and HV/VV represent the three different polarization ratios.

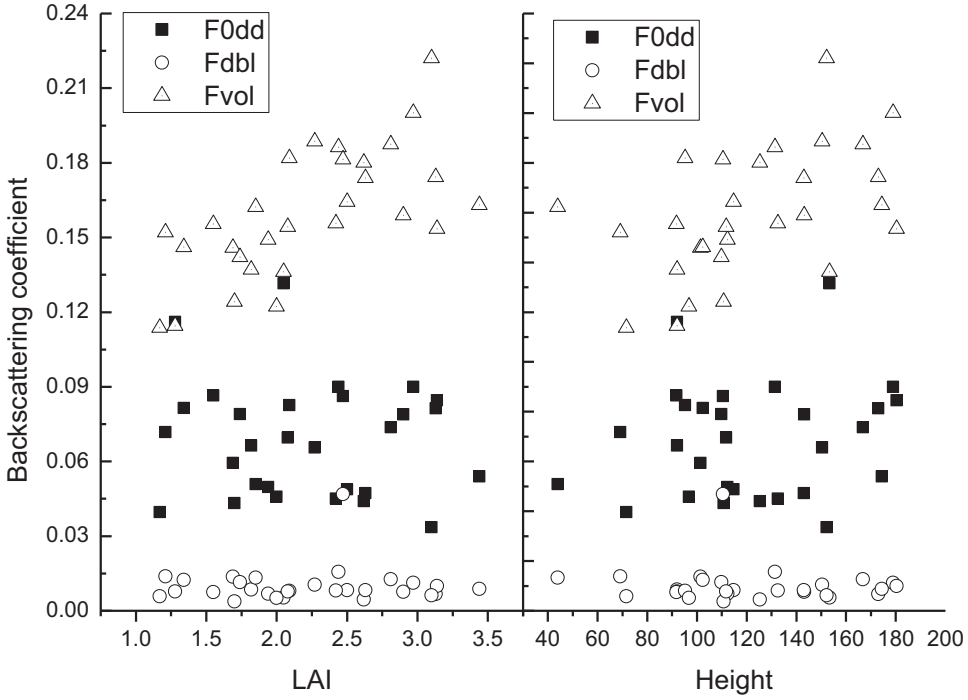

Fig. 6. Relationships between three components of Freeman–Durden decomposition and LAI, height of maize. F0dd, Fdbl and Fvol represent the single scattering, double-bounce scattering and volume scattering, respectively.

and single scattering from the stem and ground of maize plants. The LAD could reflect the orientation distributions of the structural elements of maize. With an increase in LAD (i.e., the growth of maize), the proportion of the vertical elements decreased and the VV/HH index also decreased. This phenomenon was also verified by the scattering simulation of a Scots pine shoot (Manninen et al., 2005a). Because the leaves of the maize were often curled up during a specific growth stage, the VV/HH index did not reveal higher correlations such as those for the Scots pine.

4.3. Integrated application both HJ-1 and RADARSAT-2

Based on the analysis above, the HJ-1 and RADARSAT-2 satellites were both found to be sensitive to the architecture-related variables of maize near the heading stage (Figs. 3–5). However, for dense maize coverage, a saturation phenomenon occurred in the LAI estimation using optical VIs at a special saturation point (Haboudane et al., 2004; Tang et al., 2007).

This phenomenon may be related to the lower sensitivity of the near-infrared band in dense vegetation coverage area. In contrast, radar had an advantage in monitoring dense vegetation coverage because of its penetration and sensitivity to plant structure. However, radar backscatter was complex for different polarizations, which included ground surface scatter, double-bounce scatter, and volume scatter from different parts of the plant. In this study, Freeman–Durden three-component decomposition showed that volume scattering was the main source of vegetation backscattering, and double-bounce scattering only contributed a small amount to the total scattering (Fig. 6). Usually, the largest contribution of volume scattering mainly comes from the crown, the layer between the bottom where the first green leaf exists and the top leaf of maize. Although the SAR signal was heavily affected by soil moisture during the early stage of crop growth, the effect was weakened by dense vegetation coverage (stem elongation, mean LAI = 2.2, mean height = 1.2) (Blaes et al., 2006). Other studies have also found that, for crops with LAI > 1.0, the sensitivity of the SAR signal to surface soil moisture content is substantially reduced (Moran et al., 2002). In this study, volume scattering was strongly correlated with the crown structure parameters, such as LAI and height, compared to the other two scattering types (Fig. 6). In fact, the volume scattering was also strongly related to leaf parameters, such as leaf density, leaf size, and thickness (Ulaby et al., 1990). In this context, volume scattering could be used as a good indicator to describe the growth status of a crop when the dielectric properties of the target are relatively constant. In addition, the backscattering of cross-polarization was strongly related to the volume scattering (Ulaby et al., 1986), and in the Freeman–Durden decomposition, the cross-backscattering was directly proportional to the volume scattering (Fig. 6).

As shown above, both multi-spectral and SAR satellite data had advantages in monitoring vegetation growth. The multi-spectral optical sensors could easily distinguish the green leaves and their distribution, which concern the photosynthesis of plant. Moreover, the multispectral VIs were widely used for fine vegetation classification and biophysical and biochemical parameter inversion. However, the saturation problem would become much more obvious for structure parameter inversion with crop growth. In contrast, microwaves of the appropriate wavelength and mode could penetrate the vegetation crown layer and be sensitive to plant structure. Inspired by the VIs of optical remote sensing, the microwave-modified VIs were designed to overcome the shortcomings of optical VIs for dense vegetation coverage.

Here, the commonly used multi-spectral optical VIs, such as RVI, NDVI, and EVI (Table 4), were multiplied by the cross-polarization backscattering coefficient of SAR. Then, the new VIs were obtained as the formulae (4)–(6), where HV represents cross-polarization

Table 4
Optical multispectral vegetation indices used in this study.

VI	Formula
RVI	$RVI = R_{Nir}/R_{Red}$
NDVI	$NDVI = (R_{Nir} - R_{Red})/(R_{Nir} + R_{Red})$
EVI	$EVI = 2.5 \times (R_{Nir} - R_{Red})/(1 + R_{Nir} + 6 \times R_{Red} - 7.5 \times R_{Blue})$

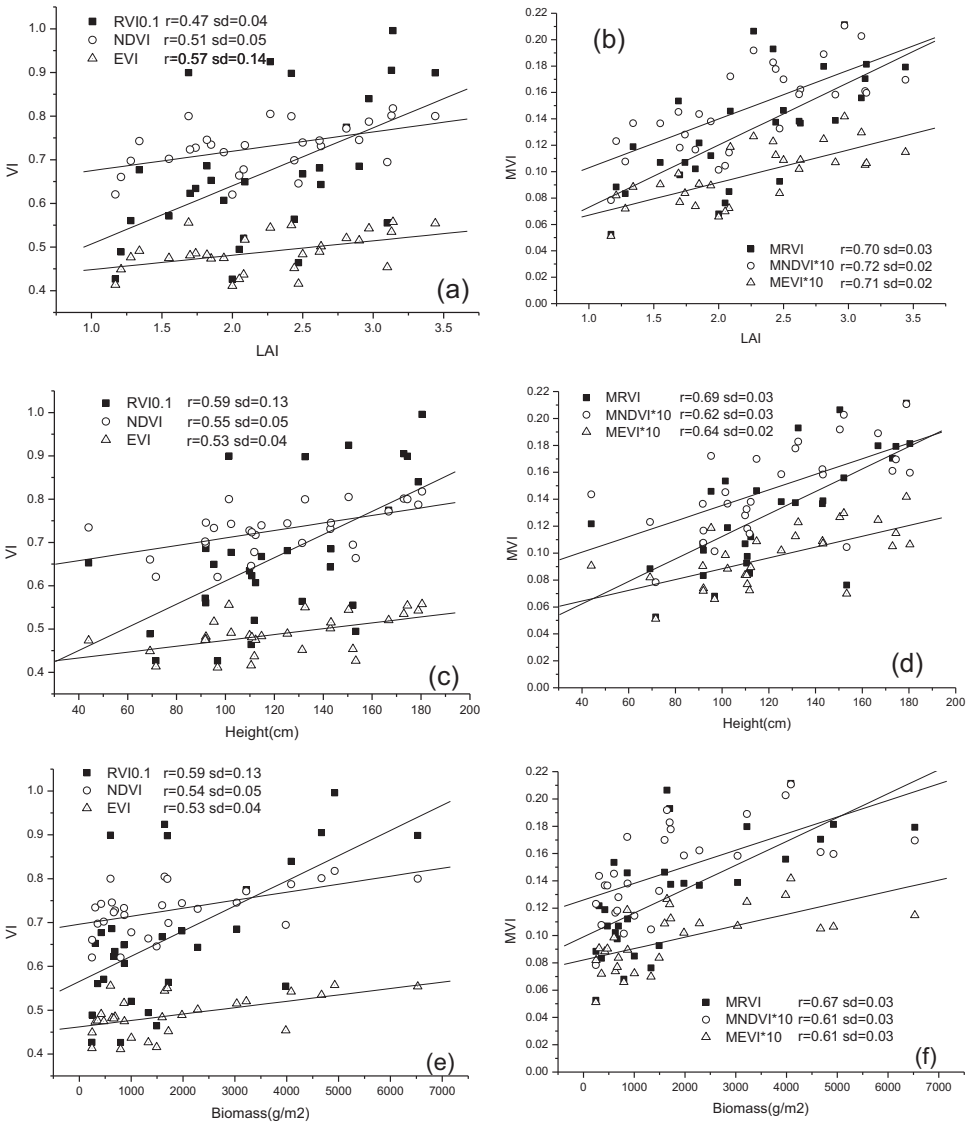

Fig. 7. Comparison between the original multispectral VI and the new integrated VIs for structure parameter inversion.

and R represents reflectance, with the subscript indicating the band. For the integrated VIs, the optical parts could distinguish the green leaves and basically estimate their amount, and the SAR parts could measure the backscatter from the crown layer. To validate those VIs' performance for structure parameter inversion, a correlation analysis was carried out.

$$\mathrm{MRVI} = \mathrm{HV} \times \frac{R_{\mathrm{Nir}}}{R_{\mathrm{Red}}} \tag{4}$$

$$\mathrm{MNDVI} = \mathrm{HV} \times \frac{R_{\mathrm{Nir}} - R_{\mathrm{Red}}}{R_{\mathrm{Nir}} + R_{\mathrm{Red}}} \tag{5}$$

$$\mathrm{MEVI} = \mathrm{HV} \times \frac{2.5 \times (R_{\mathrm{Nir}} - R_{\mathrm{Red}})}{1 + R_{\mathrm{Nir}} + 6 \times R_{\mathrm{Red}} - 7.5 \times R_{\mathrm{Blue}}} \tag{6}$$

The comparison showed higher correlation coefficients than those of the optically determined VIs (Fig. 7). The highest correlation coefficient ($r = 0.72$, SD = 0.02) was found for the relationship between LAI and MNDVI. Compared to that indicated by the analysis above, this correlation increased for the structure-related parameters, especially when they were compared to the original RVI, NDVI, and EVI. Regardless of the LAI, height or biomass of maize, all of the new VIs performed better than the original ones. Moreover, regardless of the correlation coefficients or the confidence level, the new VIs verified their potential for parameter estimation. This comparison showed that the new VIs could offer a simple and efficient way to integrate data from two different satellites.

5. Discussion

This study mainly focused on better understanding the role of the structure-related parameters of maize in their interaction with multispectral and SAR data. Compared to the leaf parameters, such as LAD, LWC and CC, multispectral HJ-1 was sensitive to the canopy characteristics of maize. However, relatively poor correlation was found between HJ-1 reflectance and the canopy parameters in the area with dense vegetation coverage. Similarly, the vegetation indices RVI, NDVI, and EVI were also not very effective for maize canopy parameter inversion in the heading stage due to near-infrared reflectance saturation.

In contrast, SAR was able to penetrate the dense vegetation coverage; therefore, theoretically, it could be used to estimate these structure parameters. However, there was a large difference between different polarization types and polarization combination. The cross-polarization was found to be directly related to the crown volume scattering intensity, which was

more highly correlated to maize structure parameters than co-polarization for maize during same growing stage. Although relevant studies have found that polarization ratios, such as VV/HH and HV/HH, are suitable for LAI estimation for some crops and forests (Manninen et al., 2005b; Dente et al., 2008; Li et al., 2009), a weak correlation was found in this study. None of these ratios revealed advantages better than that of the cross-polarization. The curly leaves of maize were considered the main reason during the specific growth stage, and the incidence angle of the SAR sensor also affected the performance (Manninen et al., 2007).

Due to the dense coverage of maize near the heading stage, the near-infrared reflectance was not strongly sensitive to the maize variables. However, the absorption feature of visible light was still obvious in the thriving stage. Constructed using both near-infrared and visible-light bands, the original multispectral VIs indicated advantages in maize growth monitoring. However, their efficiency was affected by the saturation phenomenon in dense vegetation coverage area; therefore, the active microwave sensing technique (SAR) was introduced. The Freeman–Durden three-component decomposition indicated that volume scattering dominated the SAR total backscattering interaction with maize, and it was directly related to the leaf parameters in high-coverage vegetation (Karam et al., 1992). Thus, cross-polarization was introduced in to the integrated application with multispectral data in this analysis. The optical-microwave-modified VIs were designed using the original VIs multiplied by the HV cross-polarization. Comparison showed that the new VIs had advantages in structure parameter estimation in areas of dense vegetation coverage. The coefficient of the determination reached ~ 0.7 for the relationship between the modified VIs and LAI. The better performance of the modified VIs was attributed to the stronger penetration ability of the cross-polarization of SAR. Among the three modified VIs, MNDVI had the highest potential for the estimation of structure-related parameters, while the MNDVI and MEVI were also valuable in the inversion estimation. The determination coefficient increased, and the stand error greatly decreased (Fig. 7).

In fact, there are other approaches that combine optical data with SAR to estimate vegetation parameters. Usually, optical and SAR data are used separately. Then, the results from both sensors are combined to obtain the final results. For example, the reciprocal of the standard deviation of separate estimation is usually used as a weighting factor in synergistic applications (Clevers and Vanleeuwen, 1996; Manninen et al., 2005a). Often, the optical or SAR data only offer an initial interpretation, and other data are used for more in-depth investigation (Moran et al., 2002). In this study, new VIs were designed based on the optical reflectance and SAR backscatter mechanism. This approach represents a novel synergistic way of effectively estimating vegetation structural parameters.

Although the new VIs seem better than the original ones, further tests and validation are needed before their wide application. Model simulation and field experiments are necessary, and many more important factors should be carefully considered in this process. For example, the incidence angle of SAR strongly affected the backscattering of vegetation and the L band of SAR was reported to be much more sensitive to biomass than the C band (Paloscia, 1998). Moreover, SAR backscattering was strongly affected by precipitation, and incidentally, there was 2.6 mm of precipitation on the night of July 17 during the collection of field data. These facts may introduce some uncertainties in the sampling of water-related parameters.

6. Conclusion

The new VIs determined by both multispectral HJ-1 and RADARSAT-2 satellites were found to correlate well with the structural parameters of maize near the heading stage, such as LAI and height. First, the interaction of multispectral and microwave backscattering signatures with maize canopy growth variables were analyzed. The comparative analysis clearly demonstrated the difference in sensitivity of the two sets of observational data to maize growth variables. For the HJ-1 data, the visible-light bands correlated well with these variables for light absorption during the maize growth stage. For the RADARSAT-2 data, there was an explicit correlation between the cross-polarization and these parameters. Based on the reflectance and microwave backscatter mechanism, the optical- and microwave-integrated indices were designed to overcome the disadvantage of the saturation of the original optical VIs. In fact, the validation showed that the new VIs performed better. The integrated VIs provided a good alternative to using only the optical or microwave method and presented interesting and feasible prospects.

It has been reported that many more satellite sensors, including multispectral and SAR, will be launched in the future. Thus, it will be possible to obtain two types of data on the same day. In fact, there are many passive and active sensors that are deployed in the same platform, such as ENVISAT (ESA). Therefore, the new VIs presented will probably play an important role in vegetation monitoring. This case study may be valuable in guiding further research on quantifying the different responses of optical reflectance and microwave backscatter to vegetation variables. Certainly, much work, such as model simulation and field experiments, should be conducted for proper validation and application.

Acknowledgements

Thanks to Michelle Coreena Tappertc from Earth Observation System Laboratory, Department of Earth and Atmospheric Sciences, University of Alberta, T6G 2E3, Canada for correcting the language in this paper. We also appreciate all of the suggestions and comments from the anonymous reviewers. This work was supported by the Major State Basic Research Development Program of China (2013CB733405), the National Natural Science Foundation of China (41201345), the National High Technology Research and Development Program of China (2012AA12A304) and the Special Foundation for Young Scientists of the State Laboratory of Remote Sensing Science (RC12).

References

Blaes, X., Defourny, P., Wegmuller, U., Della Vecchia, A., Guerriero, L., Ferrazzoli, P., 2006. C-band polarimetric indexes for maize monitoring based on a validated radiative transfer model. IEEE Transactions on Geoscience and Remote Sensing 44, 791–800.

Chen, J.M., Cihlar, J., 1996. Retrieving leaf area index of boreal conifer forests using Landsat TM images. Remote Sensing of Environment 55, 153–162.

Chen, J.M., Rich, P.M., Gower, S.T., Norman, J.M., Plummer, S., 1997. Leaf area index of boreal forests: theory, techniques, and measurements. Journal of Geophysical Research – Atmospheres 102, 29429–29443.

Clevers, J.G.P.W., Vanleeuwen, H.J.C., 1996. Combined use of optical and microwave remote sensing data for crop growth monitoring. Remote Sensing of Environment 56, 42–51.

Dabrowska-Zielinska, K., Inoue, Y., Kowalik, W., Gruszczynska, M., 2007. Inferring the effect of plant and soil variables on C- and L-band SAR backscatter over agricultural fields, based on model analysis. Advances in Space Research 39, 139–148.

Darvishzadeh, R., Skidmore, A., Schlerf, M., Atzberger, C., 2008. Inversion of a radiative transfer model for estimating vegetation LAI and chlorophyll in a heterogeneous grassland. Remote Sensing of Environment 112, 2592–2604.

Dash, J., Curran, P.J., Tallis, M.J., Llewellyn, G.M., Taylor, G., Snoeij, P., 2010. Validating the MERIS Terrestrial Chlorophyll Index (MTCI) with ground chlorophyll content data at MERIS spatial resolution. International Journal of Remote Sensing 31, 5513–5532.

Daughtry, C.S.T., Walthall, C.L., Kim, M.S., Colstoun, D.E., Mcmurtrey, E.B.J.E., 2000. Estimating corn leaf chlorophyll concentration from leaf and canopy reflectance. Remote Sensing of Environment 74, 229–239.

Dente, L., Satalino, G., Mattia, F., Rinaldi, M., 2008. Assimilation of leaf area index derived from ASAR and MERIS data into CERES-wheat model to map wheat yield. Remote Sensing of Environment 112, 1395–1407.

Freeman, A., Durden, S., 2002. A three-component scattering model for polarimetric SAR data. IEEE Transactions on Geoscience and Remote Sensing 36, 963–973.

Frolking, S., Palace, M.W., Clark, D.B., Chambers, J.Q., Shugart, H.H., Hurtt, G.C., 2009. Forest disturbance and recovery: a general review in the context of spaceborne remote sensing of impacts on aboveground biomass and canopy structure. Journal of Geophysical Research – Biogeosciences 114, G00E02, http://dx.doi.org/10.1029/2008JG000911.

Haboudane, D., Miller, J.R., Pattey, E., Zarco-Tejada, P.J., Strachan, I.B., 2004. Hyperspectral vegetation indices and novel algorithms for predicting green LAI of crop canopies: modeling and validation in the context of precision agriculture. Remote Sensing of Environment 90, 337–352.

Huete, A.R., Liu, H.Q., Batchily, K., Vanleeuwen, W., 1997. A comparison of vegetation indices global set of TM images for EOS-MODIS. Remote Sensing of Environment 59, 440–451.

Inoue, Y., Kurosu, T., Maeno, H., Uratsuka, S., Kozu, T., Dabrowska-Zielinska, K., Qi, J., 2002. Season-long daily measurements of multifrequency (Ka, Ku, X, C, and L) and full-polarization backscatter signatures over paddy rice field and their relationship with biological variables. Remote Sensing of Environment 81, 194–204.

Jacquemoud, S., Baret, F., 1990. PROSPECT: a model of leaf optical properties spectra. Remote Sensing of Environment 34, 75–91.

Johnstone, I.M., Raimondo, M., 2004. Periodic boxcar deconvolution and diophantine approximation. Annals of Statistics 32, 1781–1804.

Jordan, C.F., 1969. Derivation of leaf area index from quality of light on forest floor. Ecology 50, 663–666.

Karam, M., Fung, A., Lang, R., Chauhan, N., 1992. A microwave scattering model for layered vegetation. IEEE Transactions on Geoscience and Remote Sensing 30, 767–784.

Lee, J.S., Pottier, E., 2009. Polarimetric Radar Imaging: From Basics to Applications. CRC Press, Taylor&Francis Group, New York.

Li, X., Li, X.W., Li, Z.Y., Ma, M.G., Wang, J., Xiao, Q., Liu, Q., Che, T., Chen, E.X., Yan, G.J., Hu, Z.Y., Zhang, L.X., Chu, R.Z., Su, P.X., Liu, Q.H., Liu, S.M., Wang, J.D., Niu, Z., Chen, Y., Jin, R., Wang, W.Z., Ran, Y.H., Xin, X.Z., Ren, H.Z., 2009. Watershed allied telemetry experimental research. Journal of Geophysical Research – Atmospheres 114, 19.

Lu, L., Li, X., Huang, C.L., Ma, M.G., Che, T., Bogaert, J., Veroustraete, F., Dong, Q.H., Ceulemans, R., 2005. Investigating the relationship between ground-measured LAI and vegetation indices in an alpine meadow, north-west China. International Journal of Remote Sensing 26, 4471–4484.

Macdonald, D., 2008. Associates Ltd. Radarsat-2 Product Format Definition. RN-RP-51-2713.

Manninen, T., Penttil, A., Lumme, K., 2007. C-band scattering simulation of a Scots pine shoot. Waves in Random and Complex Media 17, 85–98.

Manninen, T., Smolander, H., Voipio, P., Stenberg, P., Rautiainen, M., Ahola, H., 2005a. Boreal forest LAI retrieval using both optical and microwave data of ENVISAT. IGARSS 2005. IEEE International Geoscience and Remote Sensing Symposium 7, 5033–5036.

Manninen, T., Stenberg, P., Rautiainen, M., Voipio, P., Smolander, H., 2005b. Leaf area index estimation of boreal forest using ENVISAT ASAR. IEEE Transactions on Geoscience and Remote Sensing 43, 2627–2635.

Moran, M.S., Hymer, D.C., Qi, J.G., Kerr, Y., 2002. Comparison of ERS-2 SAR and Landsat TM imagery for monitoring agricultural crop and soil conditions. Remote Sensing of Environment 79, 243–252.

Paloscia, S., 1998. An empirical approach to estimating leaf area index from multifrequency SAR data. International Journal of Remote Sensing 19, 359–364.

Tang, S., Chen, J.M., Zhu, Q., Li, X., Chen, M., Sun, R., Zhou, Y., Deng, F., Xie, D., 2007. Lai inversion algorithm based on directional reflectance kernels. Journal of Environmental Management 85, 638–648.

Tucker, C., 1979. Red and photographic infrared linear combinations for monitoring vegetation. Remote Sensing of Environment 8, 127–150.

Ulaby, F., Moore, R., Fung, A., 1986. Microwave Remote Sensing: From Theory to Applications. Artech House Publishers, Norwood, MA.

Ulaby, F., Sarabandi, K., Mcdonald, K., Whitt, M., Dobson, M., 1990. Michigan microwave canopy scattering model. International Journal of Remote Sensing 11, 1223–1253.

Ulaby, F.T., Allen III, C.T., Eger, G., Kanemasu, E., 1984. Relating the microwave backscattering coefficient to leaf area index. Remote Sensing of Environment 14, 113–133.

Zhao, M., Heinsch, F., Nemani, R., Running, S., 2005. Improvements of the MODIS terrestrial gross and net primary production global data set. Remote Sensing of Environment 95, 164–176.